

Expanded View Figures

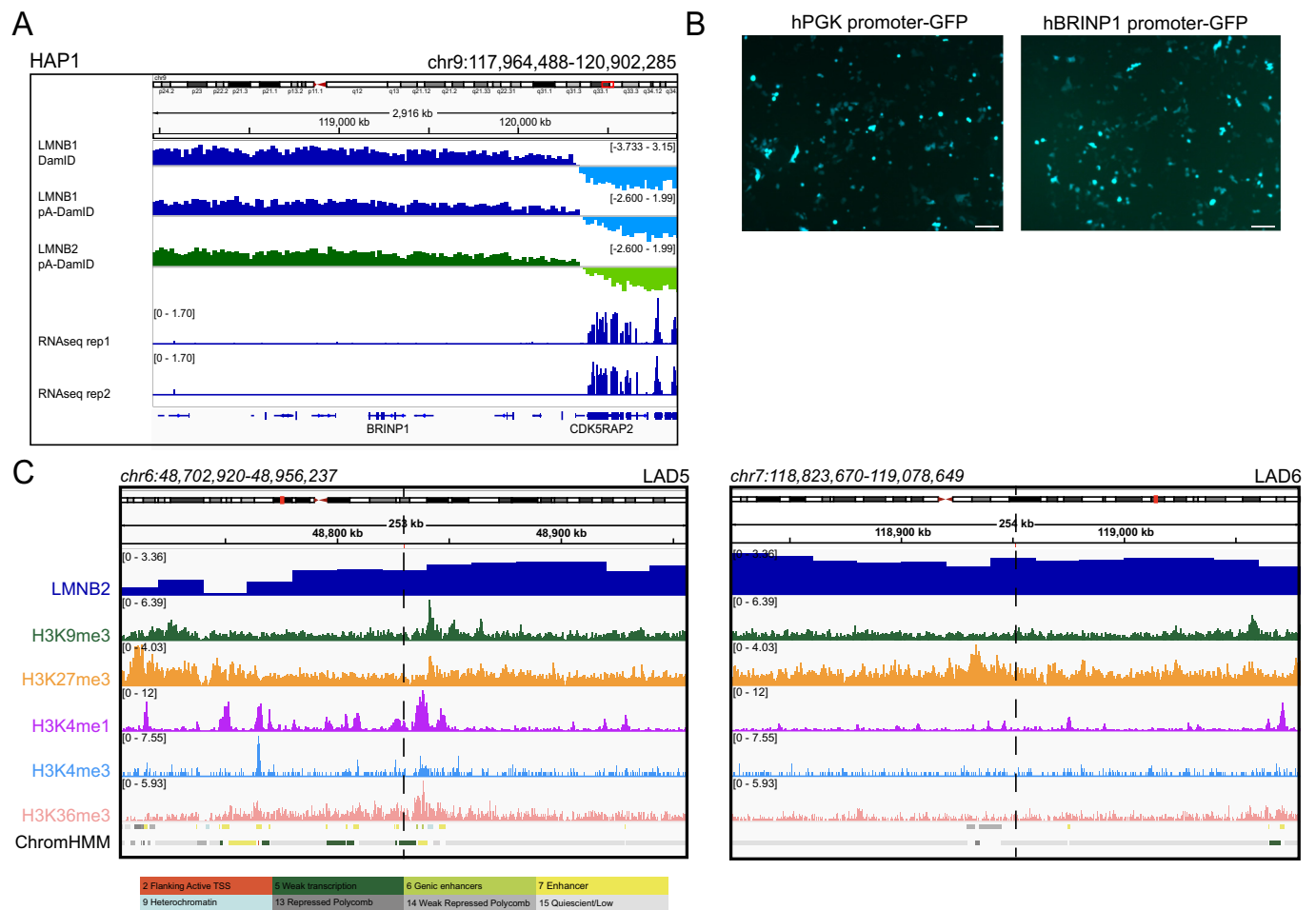
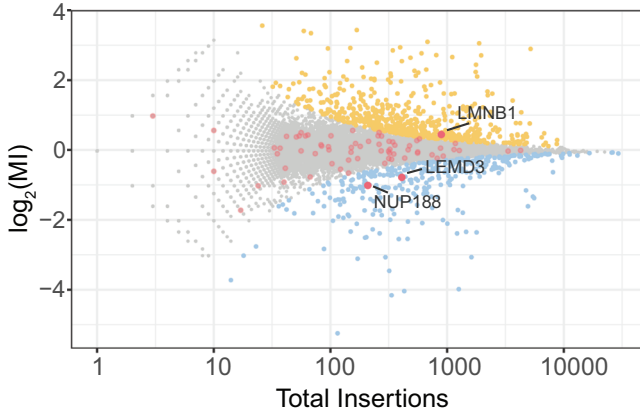


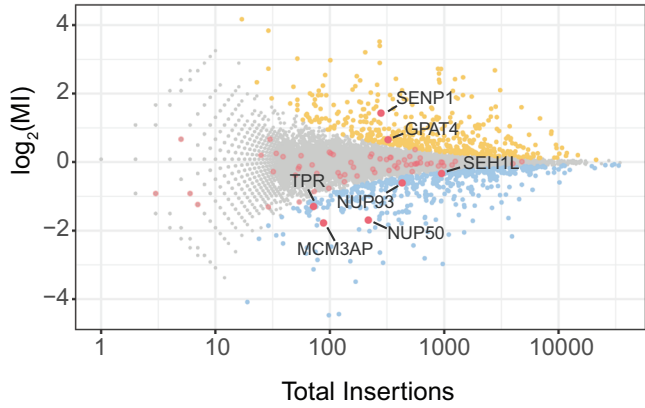
Figure EV1. Characterization of BRINP1 promoter and the chromatin environment around LAD reporters' integration sites in HAP1 cells.

(A) Top tracks: IGV tracks showing DNA-NL contacts (generated by *in vivo* DamID, LMNB1 pA-DamID, and LMNB2 pA-DamID) of 3 Mb region surrounding the BRINP1 gene. Bottom tracks: RNA-seq levels for *BRINP1* and surrounding genes in the same 3 Mb genomic regions. (B) Transfection of HAP1 cells with *phPGK::GFP* or *pBRINP1::GFP* plasmids. *BRINP1* promoter is active in HAP1 cells when expressed in an episomal setting. Scale is at 20 μ m. (C) DamID tracks for LMNB2 and ChIP-seq data for H3K9me3, H3K27me3, H3K4me1, H3K4me3, and H3K36me3 in HAP1 in a 250 kb window surrounding LAD5 and LAD6 reporter integrations (dashed lines). Data are from (Haarhuis et al, 2022). The bottom track shows annotations of major chromatin states according to ChromHMM (Ernst and Kellis, 2012); corresponding color key is shown in the bottom panel. Results are from at least two biological replicates.

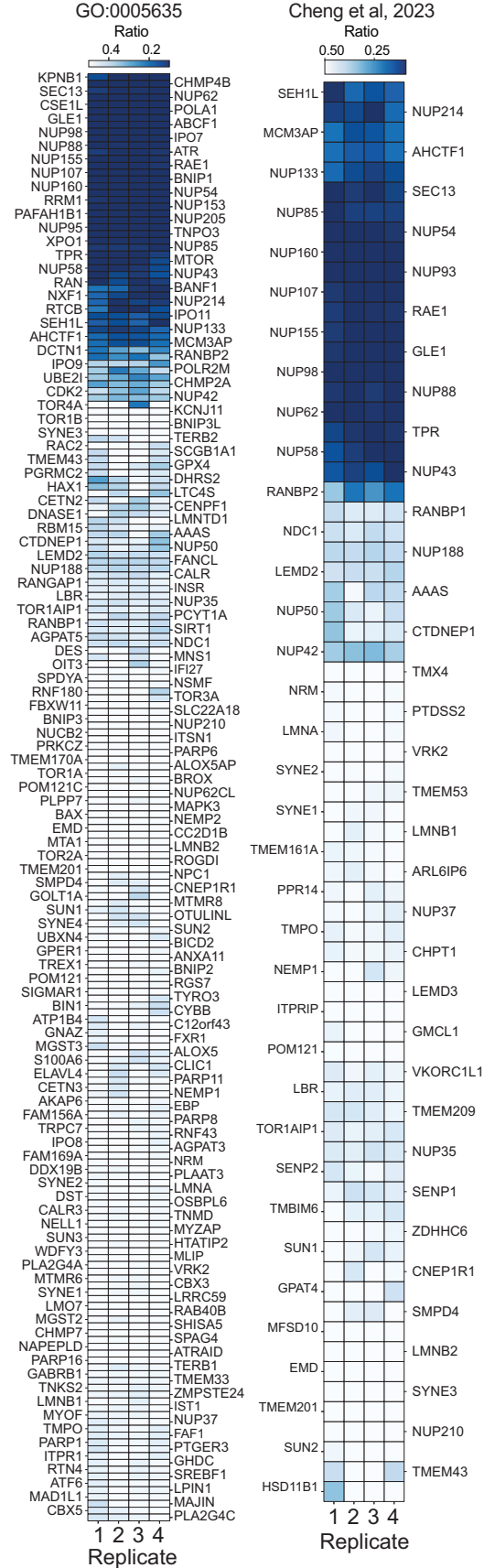
A All Nuclear Envelope Proteins in LAD5 (Cheng et al, 2023)



All Nuclear Envelope Proteins in LAD6 (Cheng et al, 2023)



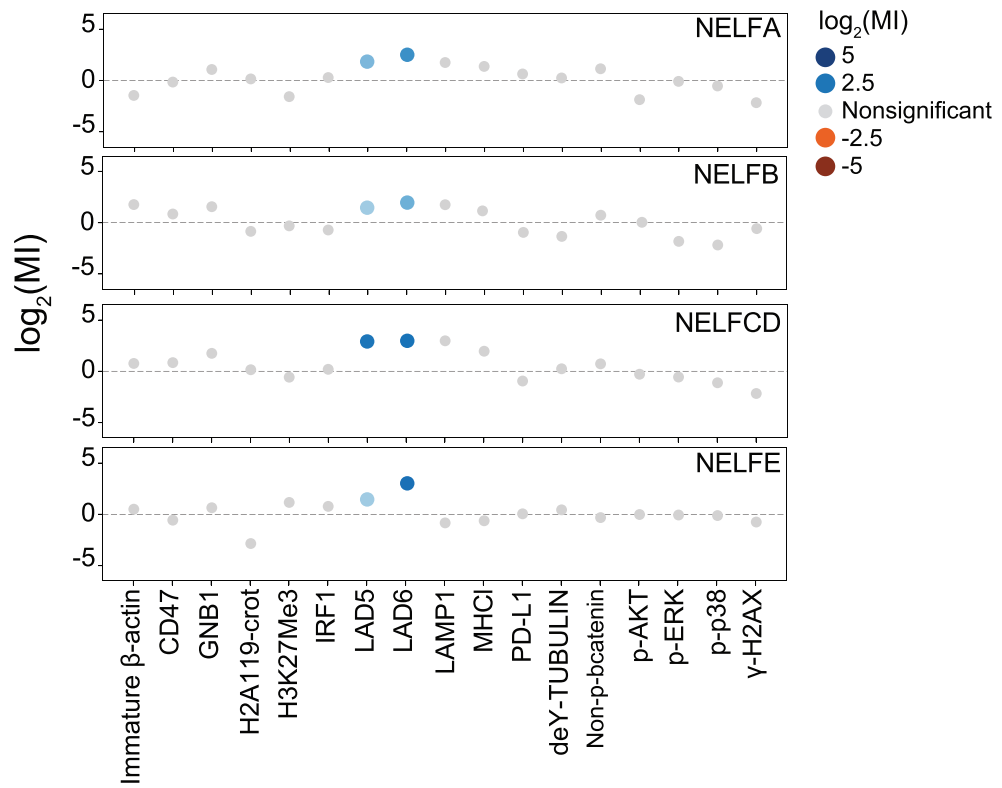
B Fitness score of Nuclear Envelope proteins



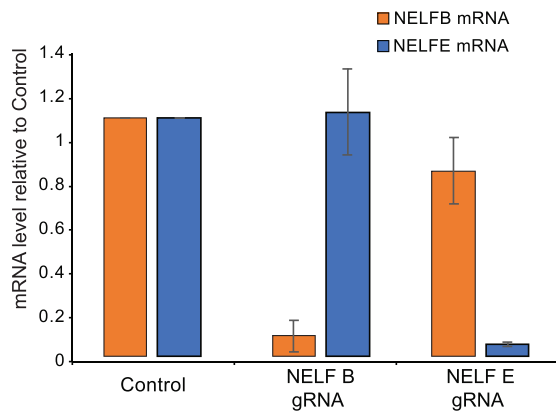
◀ Figure EV2. Nuclear Lamina genes in the screen and their essentiality in HAP1 cells.

(A) Biochemically identified NE proteins (Cheng et al, 2019) (red dots) highlighted in the screen fishtail plots for LAD5 (top) and LAD6 (bottom). The majority of these NE proteins are not significant hits in the screens. Names of the handful of significant screen hits are indicated in black. (B) Essentiality scores of proteins in GO category [GO:0005635](#) (left panel) and of proteins biochemically identified as NE proteins (Cheng et al, 2019), (right panel). Heatmaps show the ratio of sense insertions to the total insertions in wild-type HAP1 cells across 4 independent replicates under untreated conditions. Data are from (Blomen et al, 2015). The scores represent the ratio of disruptive insertions (sense) to the total insertions (sense “disruptive” + antisense “non-disruptive”) within the intronic regions of each gene. Genes crucial for cell viability will have fewer disruptive insertions as these cells are depleted, whereas cells with non-disruptive (antisense) insertions survive. As disruptive and non-disruptive integrations occur at similar frequencies, the ratio of insertions in the surviving population indicates whether a gene is important for cell fitness (Blomen et al, 2015). The lower the ratio (blue shading), the more important the gene is for HAP1 cell fitness. Results from 4 different biological replicates are shown separately.

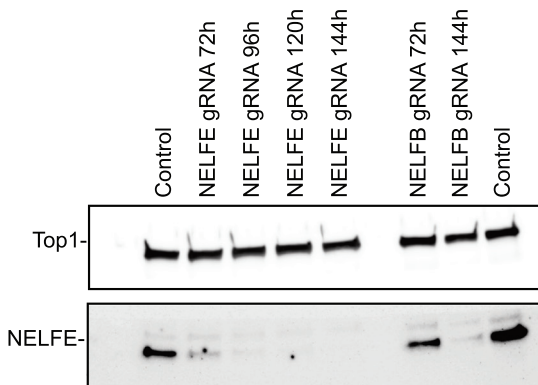
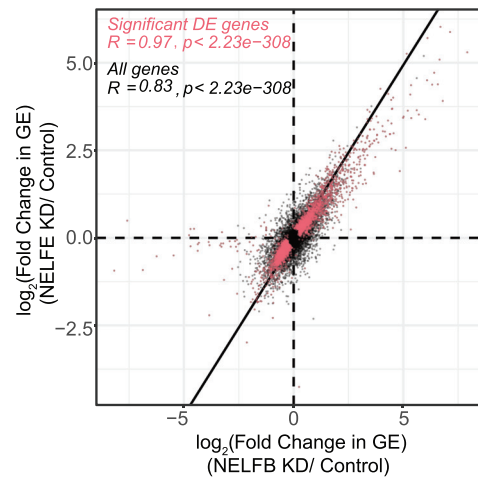
A



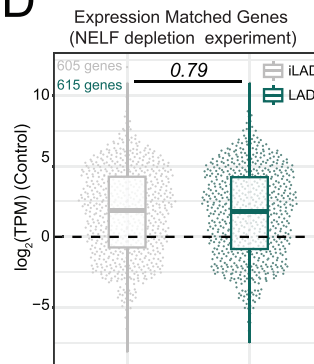
B



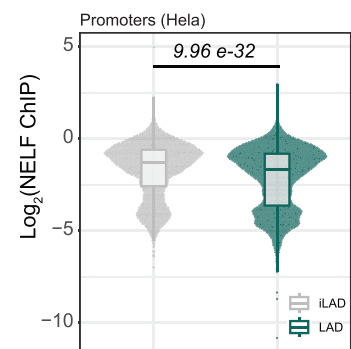
C



D



E



◀ **Figure EV3. NELF depletion in HAP1.**

(A) The mutational index (MI) for subunits from the NELF complex (NELFA, NEFLB, NELFCD, NELFE) was plotted for the current LAD5 and LAD6 screens and 15 additional FACS-based haploid screens previously conducted in HAP1 cells using the indicated readouts (blue, negative regulator; orange, positive regulator; gray, not significant) (Brockmann et al, 2017; Haahr et al, 2022; Jongasma et al, 2021; Logtenberg et al, 2019; Mazouzi et al, 2023; Mezzadra et al, 2017; Nieuwenhuis et al, 2017). (B) NELF depletion by CRISPRi in HAP1. Top panel: mRNA levels (measured by RT-qPCR) for *NELFE* and *NELFB* following CRISPRi depletion using *NELFE* and *NELFB* specific guide RNAs, 144 h after transduction. Data were first normalized on *GAPDH* mRNA and then on *NELFE/B* mRNA levels in control cells. The error bar represents standard deviation. Results were from three replicates. Bottom panel: detection of NELFE protein levels following CRISPRi depletion using *NELFE* and *NELFB* specific guide RNAs at different timepoints after transduction. DNA topoisomerase 1 (Top1) antibody was used as loading control. (C) Correlation between changes in gene expression following *NELFB* and *NELFE* knockdowns, for all (black) and significantly de-regulated genes (red). Results were from three replicates for *NELFE* depletion and two replicates for *NELFB* depletion. The black line is the diagonal. (D) Gene expression levels for expression-matched LAD and iLAD genes in the NELF depletion experiment. (E) NELFE levels at promoters of genes in LADs and expression-matched genes in iLADs in HeLa cells. CHIP-seq data are from (Beckedorff et al, 2020). Results are from two biological replicates. *P* value is according to Wilcoxon's test. For (D, E), the central line in the boxplots represents the median. The lower and upper hinges correspond to the first and third quartiles (the 25th and 75th percentiles). The upper and lower whiskers extends from the hinge to the largest or smallest values respectively no further than 1.5 * inter-quartile range. Outliers were removed only for visualization purposes. Source data are available online for this figure.

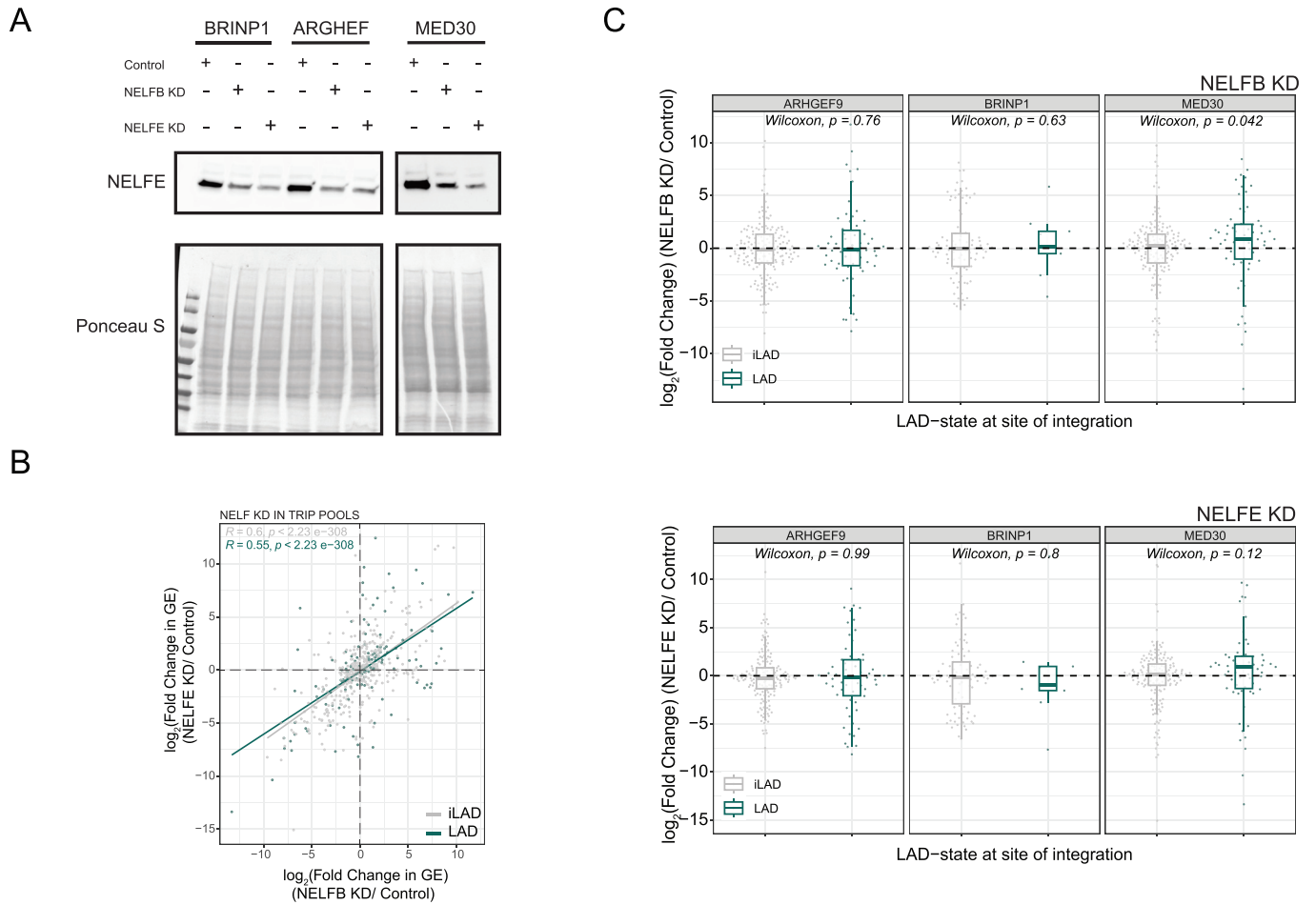
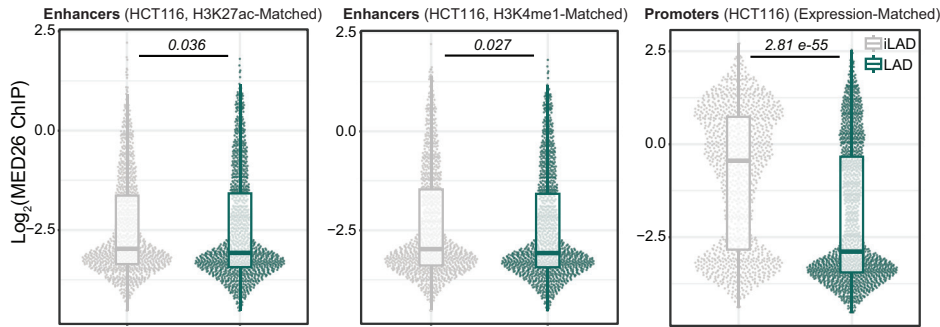


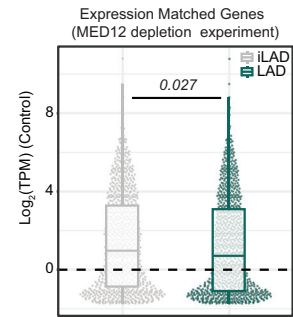
Figure EV4. NELF depletion in K562 TRIP pools.

(A–C) Multiplexed detection of the effect of depletion of NELFB and NELFE on the expression levels of reporter genes randomly integrated throughout the genome in K562 cell pools. Barcoded reporters were driven by promoters from the *ARHGEF9*, *BRINP1*, and *MED30* genes as indicated. Cell pools are from (Leemans et al, 2019). (A) Western blot of NELFE showing partial knockdown after siRNA-mediated depletion of NELFB or NELFE. (B) Changes in expression of the reporters for the three promoters throughout the genome correlate between NELFB and NELFE knockdowns. Reporters integrated in LADs are shown in green, reporters in iLADs are shown in gray. The gray and green lines represent a fitted linear model for iLAD and LAD integrations, respectively; Pearson correlation and *P* values are shown in the plots. (C) Changes in expression of each reporter (\log_2 scale) after siRNA-mediated knock-down of NELFB (top panel) and NELFE (bottom panel), divided by location in either LADs or iLADs. Results are from three replicates for P_{BRINP1} and two replicates for P_{MED30} and $P_{ARHGEF9}$. *P*-values comparing the distributions in LADs and iLADs are according to Wilcoxon test. Source data are available online for this figure.

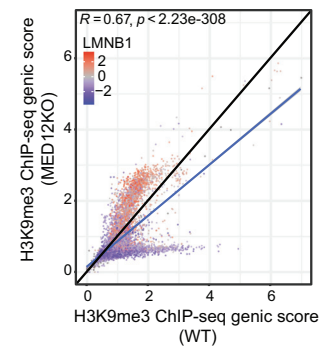
A



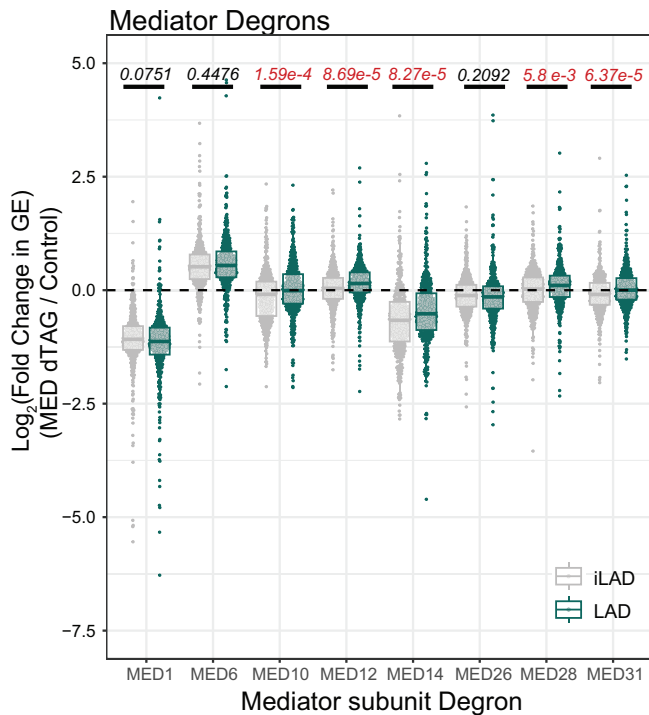
B



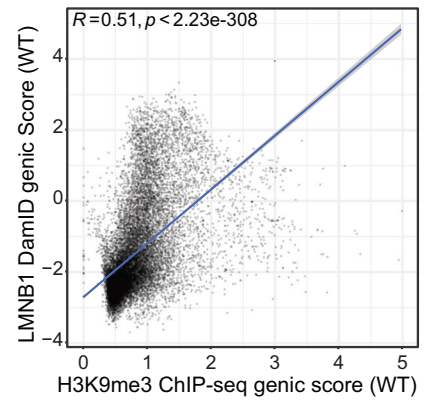
E



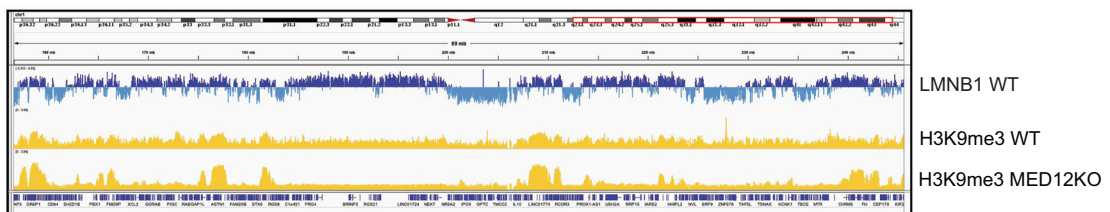
C



F



D



◀ **Figure EV5. Characterization of Mediator complex in LADs.**

(A) Top panels: MED26 binding at promoters and enhancers in HCT116 cells. Promoters were matched for TT-seq level to compare LAD and iLAD genes with similar transcriptional activity. Enhancers were matched for H3K27ac or H3K4me1 levels to compare LAD and iLAD regulatory elements with similar enhancer activity. *P* values in are according to Wilcoxon's test. Bottom panels: plot showing the similar distributions of H3K27ac (left) or H3K4me1 (middle) for matched sets of enhancers; and TT-seq levels for matched sets of promoters (right) in LADs and iLADs. Data are from two biological replicates. (B) Gene expression levels for expression-matched LAD and iLAD genes in the MED12 depletion experiments. Data are from (Haarhuis et al, 2022) and results are from 6 biological replicates. (C) Log₂(fold change) in gene expression (GE) following acute depletion of Mediator subunits for expression-matched LAD and iLAD genes. Statistical significance was calculated with Wilcoxon test for comparison of median and significant *P* values are highlighted in red. Results are from three biological replicates (D) IGV genomic tracks for 89 Mb of Chromosome 1 showing LMNB1 DamID profile for HAP1 WT (blue) and H3K9me3 ChIP-seq scores for HAP1 WT and MED12 KO (yellow). The genomic tracks show increased compartmentalization of heterochromatin in LADs following MED12 knockout. (E) Correlation between H3K9me3 levels for genes in WT and MED12 knockout cell lines. Datapoints are colored by LMNB1 DamID score. (F) Correlation between genic LMNB1 DamID score in WT and H3K9me3 levels in WT cells. The blue line (E, F) represents a fitted linear model; Pearson correlation and *P* values are shown in the plots. Results (E, F) are from three biological replicates. Data are from (El Khattabi et al, 2019; Leemans et al, 2019; Lidschreiber et al, 2021; Schick et al, 2021; Haarhuis et al, 2022, 35136067). For (A–C), the central line in the boxplots represents the median. The lower and upper hinges correspond to the first and third quartiles (the 25th and 75th percentiles). The upper and lower whiskers extends from the hinge to the largest or smallest values respectively no further than 1.5 * inter-quartile range. Outliers were removed only for visualization purposes.